Inertial instability of von Kármán street in a rotating shallow-water layer

Samuel Teinturier, Alexandre Stegner, Michael Ghil, Samuel Viboud † & Henri Didelle †

Laboratoire de Météorologie Dynamique, CNRS, Ecole Normale Superieure (ENS),
24 Rue Lhomond, 75005 Paris, France
† Laboratoire des Ecoulements Géophysiques et Industriels, Coriolis,
21 Avenue des Martyrs, 38000 Grenoble, France
teinturier@lmd.ens.fr

Abstract :

The rotation alters the stability of 2D anticyclonic flow with respect to 3D perturbations. Experiments have shown that such instability induces a transient destabilization of anticyclonic vortices in von Kármán street, when $\omega/f < -1$. However, the persistence of this selective destabilization was never studied experimentally in a shallow-water configuration. In order to investigate the impact of this vertical confinement on the inertial or the centrifugal instabilities we perform experiments on the LEGI Coriolis Platform, with a finite Rossby number, a small vertical to horizontal aspect ratio and a large Reynolds number ($Re > 5\,000$). We have shown that unstable 3D-perturbations occur for large enough Rossby number ($Ro > 0.8$) while the Reynolds number seems to control the duration of this transient instability. According to PIV measurements we have shown that, unlike the deep-water configuration, the small-scale perturbations do not reduce the local vorticity inside the unstable antiyclone. Finally, for high Rossby numbers, when the flow becomes supercritical ($Fd > 1$), due to the generation of high amplitude wave wake the vortex street intensity is significantly reduced.

Key-words :

geophysical wake ; rotating shallow-water ; instability

1 Introduction

Initially with spacecraft photography, next with sattelite imagery, clouds formation reveal vortex trails whose properties appear consistent with theories evolved with the classical von Kármán street, where cyclonic and anticyclonic vortices equally develloped (Zimmerman (1969), Thomson *et al*. (1977)). However, these vortices can have an absolute vorticity higher than the planetary vorticity, and in some cases the anticyclonic structures are distorted and less circular than their cyclonic counterpart. Some instability criteria were studied for the inviscid flows in rotation. Johnson (1963) established the criterion of the free-shear flow instability in a rotating frame which states that instability occurs when $\Phi = 2\Omega_0(2\Omega_0 + \omega) < 0$. Mutabazi *et al*. (1992) extended the classical Rayleigh criterion for centrifugal instability to rotating flows. This generalized Rayleigh criterion predicts that instability occurs when $\Phi = 2(\Omega_0 + V/r)(2\Omega_0 + \omega) < 0$. Several experimental studies showed that intense anticyclonic vortices (with the relative vorticity ratio $|\omega/2\Omega_0| > 1$) experience a transient 3D destabilization while the cyclones remain always stable and coherent (Hopfinger *et al*. (1982), Boyer *et al*. (1984), or Stegner *et al*. (2005)). These 3D perturbations diffuse the vorticity and the restabilization of the antyclonic vortices occurs after one or two inertial periods, when $\mathrm{Ro} \simeq 1$.

However, those experiments has been realised with a large aspect ratio $\alpha = h/D \sim 10$ (h, height of water ; D, diameter of the obstacle). In an atmospheric context where $\alpha \ll 1$, one can ask oneself whether the 3D inertial and elliptic instabilities still persist and how will the structure of the perturbation, namely, the vertical wavelength, will be affected by the small aspect ratio constraint. The aim on this work was to perfom several experiments on a two

layer system, with a small vertical to horizontal aspect ratio ($\alpha \sim 1/10$). This parameter range implies the use of a large tank, like on the Coriolis platform.

2 Physical parameters and Experimental sketch

In order to study instabilities in shallow-water vortex street on a rotating frame, we performed several experiments on the 14-m-diameter Coriolis rotating platform of LEGI, Grenoble. In practice we used a Coriolis parameter $f = 2\Omega_0 = 0.04$ and 0.08 rad.s^{-1}. The tank was filled with two layers of different densities, H $= 55$ cm and $\rho_1 \simeq 1005$ kg/l for the lower layer of salt water, and h $= 5$ cm and $\rho_2 \simeq 999$ kg/l for the upper layer of fresh water (Fig. 1). The reduction gravity is defined by $g^* = g\rho/(\rho_1 + \rho_2)$. The cylinder was towed in the upper layer. The wake is then confined in this shallow-water layer, the lower layer is neutral and strongly reduces the bottom friction in the upper layer.

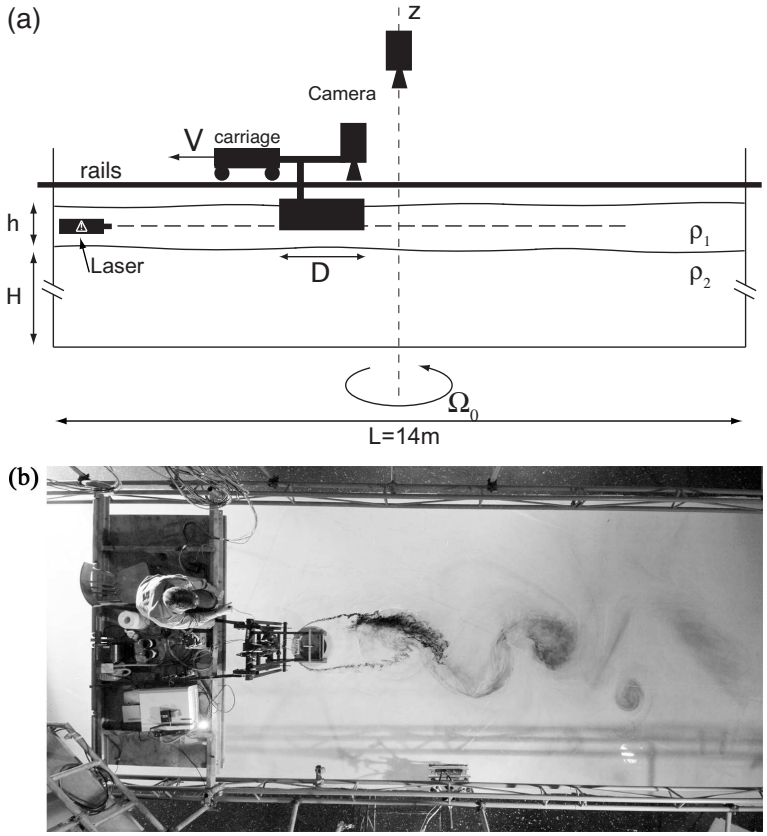

Figure 1: Side view (a) of the experimental sketch : the 2-layer system, the position of the cylinder and the cameras. Top view (b) of an experiment.

Therefore, according to dimensional analysis, with D the diameter of the obstacle, V the cylinder velocity, and in addition to the vertical to horizontal aspect ratio $\alpha = h/D$, we introduced the Rossby number Ro $= V/\Omega_0 D$, the Reynolds number Re $= VD/\nu$, and the Froude number Fr $= V/\sqrt{g^* h}$.

3 Dye observations

We performed a series of experiments varying the Rossby number (Ro $= 0.5 - 3$), with various cylinder speed V. The Reynolds number varied in the range Re $= 2000 - 30\,000$. Two dye tracer of different colors was released in amont of the cylinder boundary layer : a red dye where the vorticity was positive, and a black dye where the vorticity was negative, in order to find the red and black dyes respectively in the cyclonic and anticyclonic vortices. Three typical wake patterns have been observed, they are shown in Fig.2. We observed in the lee of the cylinder, the shedding of stable and coherent cyclones and anticyclones (Fig.2(a)). After a transient elliptical shape, the structures became quickly circular and the dye remained concentrated in the center for a long time. For Ro larger than a certain value (Ro $\gtrsim 0.8$), the black dye exhibited strong spatial perturbations inside anticyclonic structures, as shown in Fig.2(b).

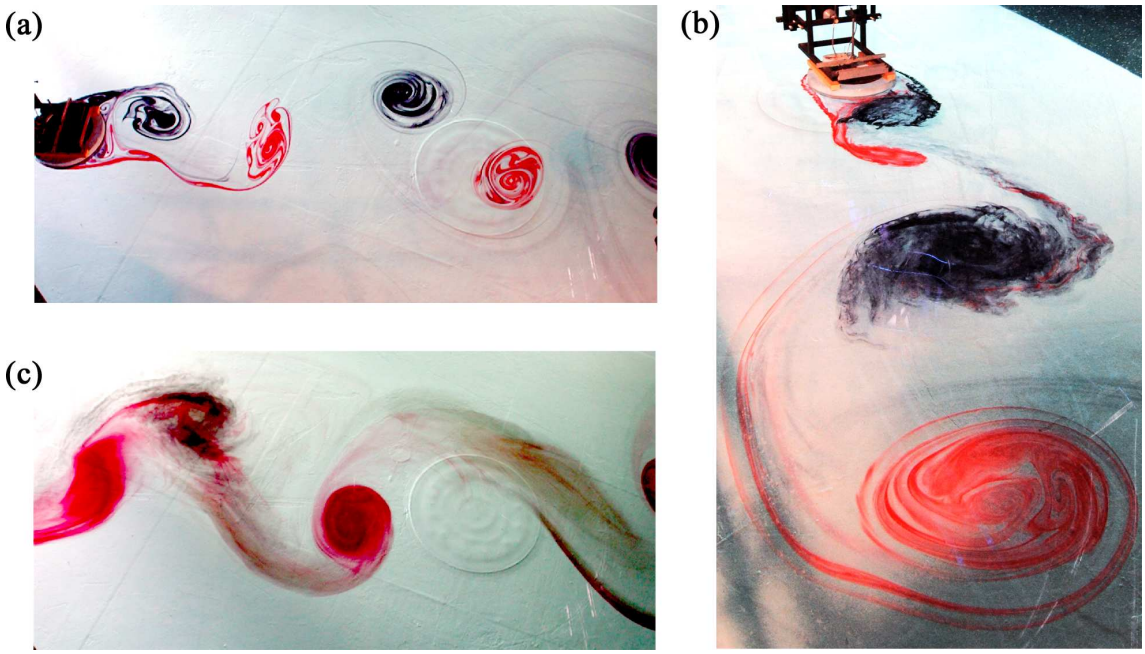

Figure 2: Examples of experiments with dye : (a) a symmetrical case for Ro≃0.4, and Re≃4000 (the cylinder moves from right to left) ; (b) front-view of an intermediate case for Ro≃1, and Re≃10000 ; (c) a strongly assymetric case, for Ro≃2, and Re≃20000, approximately 60 seconds after the passage of the cylinder ; the red and black dyes are released respectively into the cyclonic and anticyclonic part of the boundary layer of the cylinder.

Moreover, the anticyclonic vortices are systematically strongly stretched and even sometimes splitted for a large Re (Re $\gtrsim 15\,000$). Nevertheless, the latter or the splitted vortices recover their symmetrical shape after several inertial periods (typically 4 or 5). Then we can define three areas, represented schematically Fig.3.

We should notice two things here. On one hand, passive tracer observation should always be taken with care. Indeed, streaklines (i.e., the dye patterns) which integrate the history of the flow field cannot be compared to the streamlines, an instantaneous representation of the velocity field. On the other hand, the Ro considered is not calculated from the vorticity, but estimated with the forcing parameters. Only quantitative measurements like the PIV (Particle Image Velocimetry), give access to dynamic Ro $= \omega/f$, which is used for the stability criteria (cf. §1).

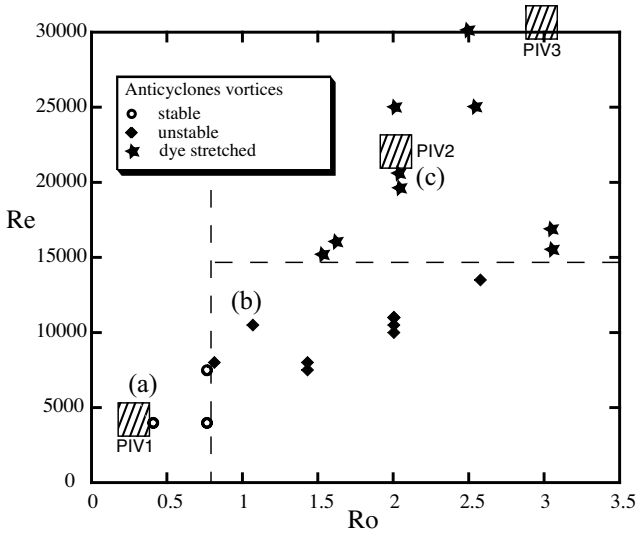

Figure 3: Diagram (Re–Ro) of all dye experiments, with three roughly delimited parts. Stability of the anticyclonic vortices in the parameter space (Re–Ro), with three roughly delimited parts. $Fr < 1$ everywhere, except for the PIV3 experiment ($Fr \simeq 1.1$). (a), (b), (c), refer respectively to Fig.2(a), (b), (c).

4 PIV measurements

In addition to dye visualization, we made quantitative measurements of the horizontal velocity field using standard PIV. Unfortunately, only few of them enable us to accurately calculate the vorticity ω. We measured the vorticity for a perfectly symmetrical wake like in the Fig.2(a). The relative vorticity filed measurements are shown in Fig.4, where ω is lower than $f/2$: the maximum values of ω/f are of approximately 0.3 and -0.3. The vortices are circular and they are of equal intensity and size ($\sim D$) for both anticyclones and cyclones.

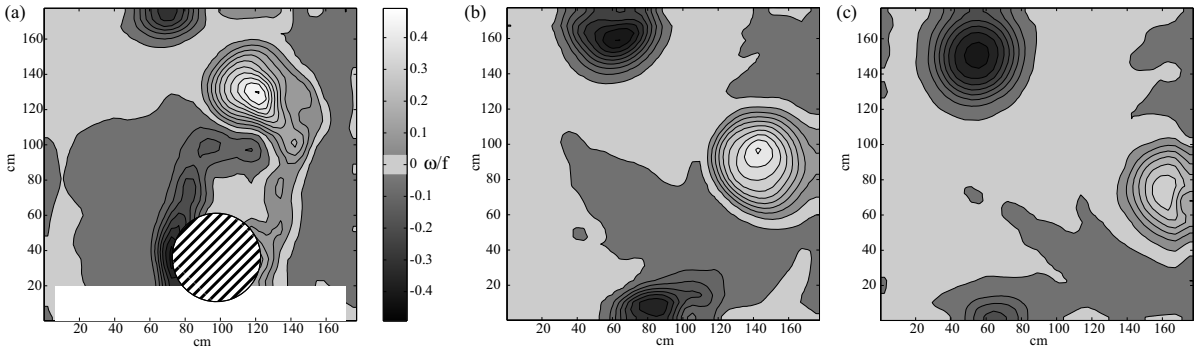

Figure 4: Relative vorticity ω/f obtained from PIV measurements of PIV1 experiment (Ro $\simeq 0.4$, Re $\simeq 4\,000$), at $t = 0$ (a), $t = 500$ (b) and $t \simeq 1\,500$sec (c). The gray-scale table is the same for the two images, and each isolines are separate by 0.05 unit.

Then, for an asymmetrical street, like in the Fig.2(c) case, the relative vorticity measurements for two vortices are shown in Fig.5(a). Unlike deep water case, $|\omega/f|$ is larger than 1.5 for several inertial periods (typically 4 or 5) for both anticyclones and cyclones. We do not obtain the same patterns as for those with dye experiments : in particular, the vorticity field does not present a stretching as on the Fig.2(c). The vorticity is an active tracer, and measures

the instantaneous dynamics of the fluid layer, unlike the dye which is a passive tracer. Moreover, due to the precision of the PIV system, it is very difficult to obtain a vorticity field which can resolve accurately the small-scale 3D perturbations seen with the dye. Nevertheless, with a specific treatment, on instantaneous velocity fields, we can distinguish some non-axysymetric perturbations of the isovorticity lines as on Fig.5(b).

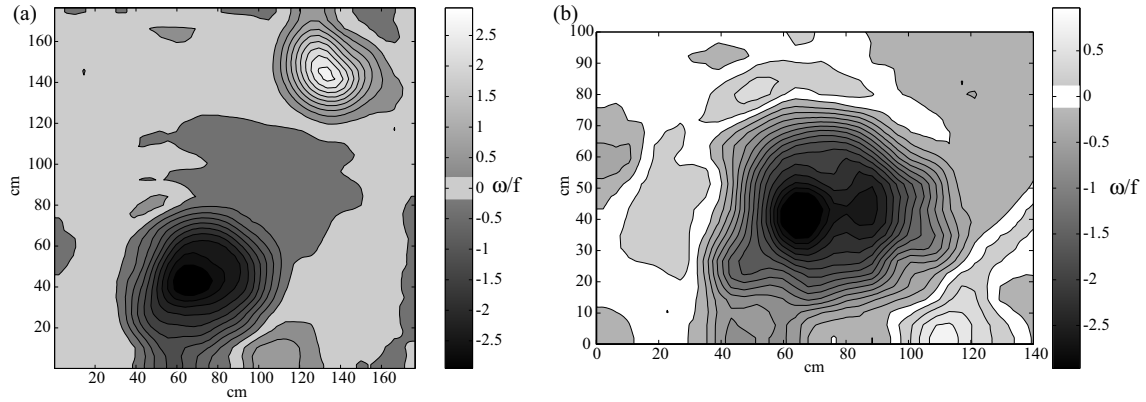

Figure 5: Relative vorticity ω/f of PIV2 experiment (Ro $\simeq 2$, Re $\simeq 20\,000$), at $t = 60$sec after the passage of the cylinder (a), each isolines are separate by 0.3 unit ; zoom of the anticyclonic vortex at approximately the same time, with a more accurate treatment and no temporal average, each isolines are separate by 0.2 unit.

Lastly, we have made supercritical flow experiments, i.e. for a Froude number Fr higher than one. We measured the velocity field on each side of the obstacle. These wake waves can be compared with recent experiments performed by Johnson *et al*. (2006). An example of these patterns for Fr $= 1.1$ is represented on Fig.6(a). The energy transmitted by these waves is not negligible, since the maximal vorticity signal is close to $f/2$. Then, vortices are formed further behind the cylinder, and their maximum vorticity is weaker than the subcritical cases, since ω is roughly equal to Ro$/3$.

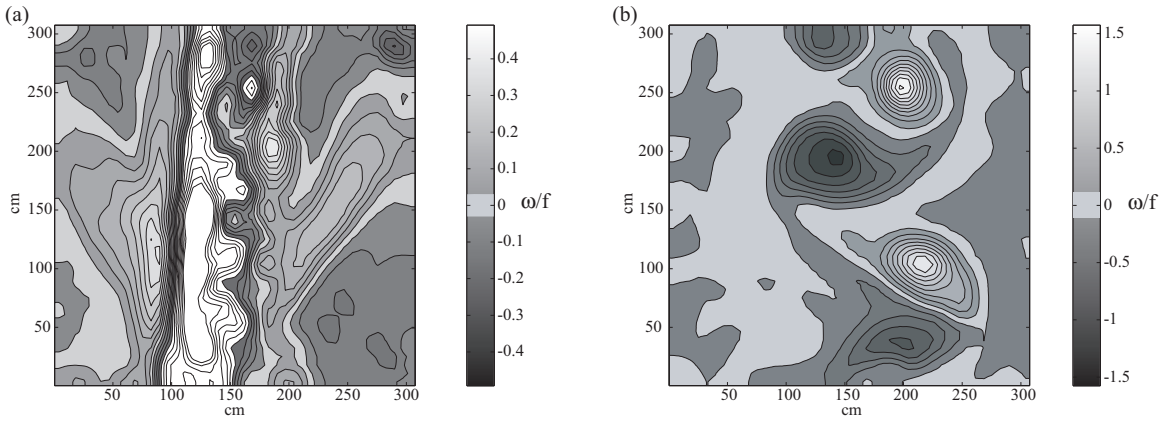

Figure 6: Relative vorticity ω/f of PIV3 experiment (Ro $\simeq 3$, Re $\simeq 30\,0003$, and Fr $\simeq 1.1$), at $t = 30$sec after the passage of the cylinder (a), with an interval of value to visualize the waves of the wake ; at $t = 160$sec at the same place.

5 Conclusions

The purpose in this work was to investigate by means of laboratory experiments the influence of shallow-water configuration on three-dimensional destabilization of rotating von Kármán streets. With dye visualisation and PIV measurments, we established a (Ro-Re) parameter diagram, and we measured the vorticity in the core of the vortices. These experiments have shown that, the 3D instability persist in a shallow-water configuration. The vertical wavelength of the perturbations, much smaller than the cylinder dimension, is not yet indentified, but it plays an important part in the vertical mixing. This confinement effect is relevant to atmospheric flows, but it could also be applied to oceanic flows. Moreover, the Reynolds number seems to play an active part in the symmetry loss of the von Kármán street in this case. For high enough Reynolds number, the anticyclones and cyclones vortices have values of ω quite higher to f for several rotation periods, unlike the deep water configuration. With a constant Ro larger than 0.8, and for a small Re, one can ask if the transient instablity still exists. Lastly, we measured the importance of the energy transfer in wave wake for vortices in supercritical flow.

References

Boyer, D. J., Kmetz, M., Smathers, L., Chabert d'Hieres, G., Didelle, H. 1984 Rotating open channel flow past right circular cylinders. *Geophys. Astrophys. Fluid Dyn.* **30** 271

Hopfinger, E. J., Browand, F. K., Y. Gagne, Y. 1982 Turbulence and waves in a rotating tank. *J. Fluid Mech.* **125** 505

Johnson, J. A. 1963 Stability of shearing motion in rotating fluid. *J. Fluid Mech.* **17** 337

Johnson, E. R., Esler, J. G., Rump, O. J., Sommeria, J., Vilenski, G. G. 2006 Orographically generated nonlinear waves in rotating and nonrotating two-layer flow. *Proc. R. Soc. A* **462** 3

Mutabazi, I. C., Normand, C., Wesfreid, J. E. 1992 Gap size effects on centrifugally and rotationally driven instability. *Phys. Fluids A* **4** 1199

Stegner, A. ,Pichon, T., Beunier, M. 2005 Elliptical-inertial instability of rotating Karman vortex streets. *Phys. Fluids* **17** 066602

Thomson, R. E., Gower, J. F. R., Bowker, N. W. 1977 Vortex streets in the wake of the Aleutian Islands. *Mon. Wea. Rev.* **105** 873

Zimmerman, L. I. 1969 Atmospheric wake phenomena near the Canary Islands. *J. Appl. Met.* **8** 896